The International Journal of Advanced Manufacturing Technology (2018) 99:127–136
https://doi.org/10.1007/s00170-018-2504-x

ORIGINAL ARTICLE

Polyethylene friction stir welding parameter optimization and temperature characterization

Shayan Eslami[1,2] · J. Francisco Miranda[2] · Luis Mourão[3] · Paulo J. Tavares[1] · P. M. G. P. Moreira[1]

Received: 24 January 2018 / Accepted: 20 July 2018 / Published online: 1 August 2018

Abstract
The use of friction stir welding (FSW) to join thermoplastics has proven to produce strong welds with good surface quality when compared to conventional welding methods. In this study, a Teflon stationary shoulder was developed to weld 3-mm-thick plates of high molecular weight polyethylene in butt-joint configuration. Different sets of welding parameters were chosen and tested to evaluate their effect on the weld strength. Also, in order to increase joint performance, the temperature generated during welding was measured. For that purpose, thermocouples were located underneath of the weld nugget surface to measure the generated frictional heat for different tool diameters and parameters. Tool diameter and rotational and welding speeds are the most influential parameters regarding the welding temperature; however, all the input parameters had statistically significant effect on the weld quality. Unlike FSW in metals, using this tool, the heat is generated mainly by surface contact of the rotating probe and copper sleeve than the base material. The strongest welded joint was able to withstand 97% of the force that is necessary to fracture the base material, without using an external heating source.

Keywords Friction stir welding (FSW) · Polyethylene · PE · Taguchi · ANOVA · Welding temperature

1 Introduction

Reducing vehicle weight by using light materials with good mechanical properties is an effective way to reduce emissions, which is essential to reduce the impact of the transport industry on the environment. Consequently, industrial demands of using polymers and composites are increasing, and so does the quest for better joining techniques. Friction stir welding (FSW) is a welding technology developed at The Welding Institute (TWI) to join aluminum alloys [1]. Initially, the FSW technique was used to weld aluminum alloys that are difficult to weld using conventional welding methods. However, the advantages of FSW technique attracted researchers to investigate the possibility of welding non-metallic materials [2]. Compared to the metallic materials, scarce research have been published for joining polymers and composites, and the literature is still lacking a tool design which is easy to manufacture, without additional heat input, making it cost effective while producing sound welds regardless of polymeric parent materials' characteristics [3].

In this process, a rotating tool with a specially designed probe and shoulder inserts into the weld materials and traverses along the weld line under the axial force, as illustrated in Fig. 1. Depending on the weld materials, it might be necessary to use dwell time at the beginning of the welding process to allow the parent material and welding tool to reach the anticipated temperature [5]. Design of the welding tool plays a fundamental role in this process, and it varies with respect to the parent materials' characteristics, geometry, and welding configuration [3]. As shown in Fig. 1, for welding polymers, a welding tool with a stationary shoulder is required to obtain sound welds [6].

The advantages of the FSW method are not limited to the weld quality and its benefits can be extended to economical aspects and environmental impact [6, 7]. Some of the FSW advantages are good repeatability and dimensional stability,

✉ Shayan Eslami
seslami@inegi.up.pt

[1] INEGI – Institute of Science and Innovation in Mechanical and Industrial Engineering, 4200-465 Porto, Portugal

[2] Departamento de Engenharia Mecânica, Faculdade de Engenharia da Universidade do Porto, Rua Dr. Roberto Frias, 4200-465 Porto, Portugal

[3] ISEP, Instituto Superior de Engenharia do Porto, Rua Dr. António Bernardino de Almeida, 431, 4200-072 Porto, Portugal

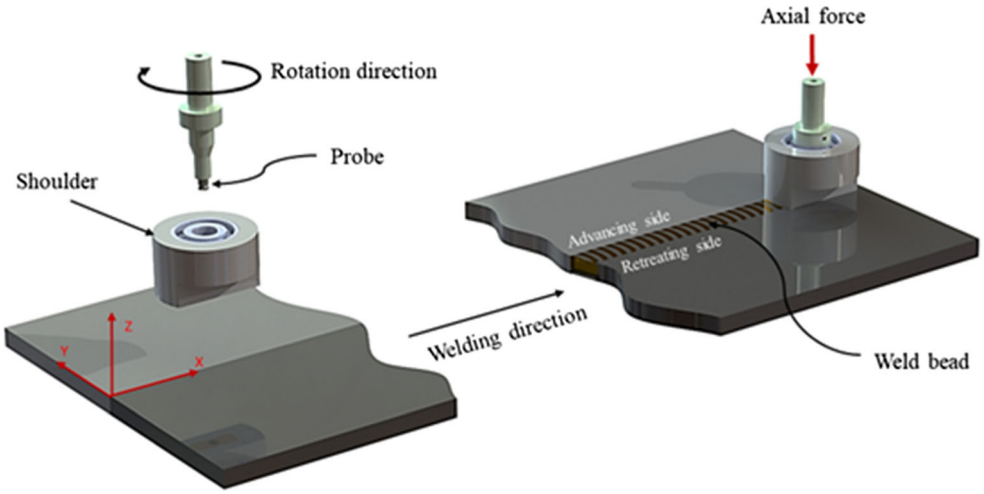

Fig. 1 FSW process in butt-joint configuration using stationary shoulder [4]

low distortion [8], applicable to a wide range of thicknesses in different configurations, highly an energy efficient process [9], improved cosmetic appearance without loss of alloying elements, no shielding gases or toxic fumes are generated, no need for the third party materials, and defects like porosity and hot cracking are not an issue in this process [10].

Although the FSW concept in metallic materials does not differ from the one employed in polymers, chemical and physical differences between these materials dictate an alternative approach in tool design. Contrary to metallic materials, due to the molecular structure and low thermal conductivity and friction coefficient of polymers, heat generation and heat transfer are drastically reduced. As a result of these differences, conventional FSW tools are not suitable to weld polymers due to formation of flash defect, which is corresponding to the ejection of the soften materials outside the weld bead [2]. To avoid formation of flash defects and produce sound welds, stationary shoulder is essential to push the material down to the weld nugget. However, using non-rotatory shoulder, the process suffers from inadequate frictional heat, which needs to be compensated by appropriate tool design and process optimization to obtain an optimum weld temperature with sound mechanical properties.

Previous studies proved that temperature has a main effect on the weld quality and its value determines the joint strength, residual stress, and distortion of the workpiece [11], which can be improved using appropriate tool designs and optimum welding parameters [12]. The mechanical properties of the fabricated joints are strongly affected by multiple defect formations and microstructure developments, which are related to temperature distribution and material flow during welding. It was claimed that the rotational speed is a crucial factor that affects directly on the welding temperature and the tensile fracture mode. The welded aluminum alloy is subjected to more ductile fracture mode using higher rotational speed, when compared with joints produced at lower rotational speed [13]. Therefore, accurate temperature measurement is crucial to predict and comprehend the optimal welding parameters.

To analyze the welding parameters influence on the joint efficiency, investigators typically follow a conventional experimental procedure, by changing one parameter at a time, which leads to an experiment where all possible combinations are tested. This conventional parametric approach requires excessive resources and it is a time-consuming process. In order to save time and cost by reducing the number of experiments, new models can be employed to extract the desired output variables more efficiently [14]. The Taguchi method is a statistical approach that uses orthogonal array to study the entire parameter range, which decreases the number of tests in an experimental design [15].

The main objective of this study was to find the optimal set of welding parameters to weld a commercially available polymer in butt-joint configuration. Different sets of welding parameters were tested following the selected Taguchi's orthogonal array to determine the optimal process parameters, and welding temperature was recorded for a better understanding of the generated frictional heat during the process.

2 Experimental procedures

Three-millimeter-thick high molecular weight polyethylene (HMW-PE) plates were welded in butt-joint configuration

Table 1 FSW process parameters and levels

Welding Parameters (unit)	Level 1	Level 2	Level 3
Tool diameter (mm)	3	4	5
Rotational speed (rpm)	1500	2000	2500
Welding speed (mm/min)	30	50	70
Axial Force (N)	800	950	1100

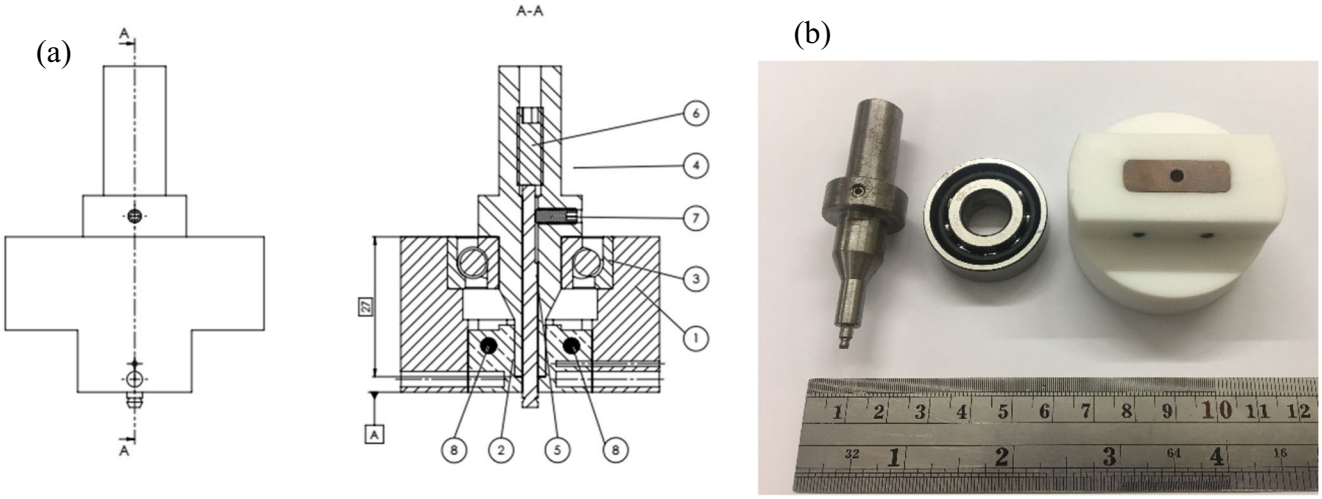

Fig. 2 Detailed view of a tool assembly (**a**) and the actual welding tool (**b**)

using a three-axis milling machine. The chosen base material for this study had a density of 0.96 g/cm^3, a melting temperature range of 130–135 °C, and a thermal conductivity of 0.41 W/mK. The axial force during welding was recorded with four load cells connected to a data acquisition system. In order to relate the vertical position command to the force actually applied to the spindle, a height setup calibration procedure was adopted [4]. A three-level Taguchi L9 orthogonal array design with the following four parameters was chosen: tool diameter, axial force, welding speed, and rotational speed [16]. The range of the values for each welding parameter and fixed parameters was defined from preliminary tests and can be seen in Table 1. These values were selected with respect to the sleeve sizes and their heat generation capacities. The parameter range was chosen in a way that all the welding conditions are able to produce acceptable joints.

The tool used in this study consists of a stationary shoulder made of Teflon with an angular contact bearing that allows independent rotational movement between the rotating probe and the shoulder. An innovative designed copper sleeve is used around the rotating probe to generate heat and compensate lack of the generated heat due to the absence of a rotatory shoulder. The frictional heat generated between the copper sleeve and the rotating probe preheats the base material before passing of the tool. For welding 3-mm PE materials, 2.95-mm-probe length and double-grooved probes with diameters of 3, 4, and 5 mm, and flat surfaces at the tips were used. The cross-sectional view of the FSW tool is illustrated in Fig. 2: Teflon stationary shoulder (1); a high thermal conductive sleeve (2); angular contact bearing (3); tool stand (4); probe with flat surfaces (5); threaded pin (6); flat point headless screw (7); and locking shafts (8). To avoid any vertical movement under the pressure, two locking shafts were used to fix the copper sleeve onto the shoulder to avoid any unwanted movement under the pressure during welding. In order to measure the generated heat on the copper sleeve, a thermocouple was inserted inside the drilled hole into the shoulder and sleeve. Using this tool, most of the frictional heat is generated and transferred to the base materials by the copper sleeve, while the probe stirs the soft materials under the axial force. The generated heat was measured inside the copper sleeve, as close as possible to the rotating probe.

In order to reduce the number of experimental tests, a L9 Taguchi orthogonal array was used to cover all the parameter ranges in nine sets of parameter combinations. The experimental conditions for the four welding parameters as inputs,

Table 2 Experimental conditions for Taguchi L9 design

Specimen number	Friction stir welding process parameters			
	Tool diameter (mm)	Rotational speed (rpm)	Welding speed (mm/min)	Axial force (N)
S1	3	1500	30	800
S2	3	2000	50	950
S3	3	2500	70	1100
S4	4	1500	50	1100
S5	4	2000	70	800
S6	4	2500	30	950
S7	5	1500	70	950
S8	5	2000	30	1100
S9	5	2500	50	800

Table 3 Tensile properties of the parent material (HMW-PE) [16]

Test results	Maximum load (N)	Maximum stress (MPa)	Young's modulus (GPa)
Mean	921.7	23.6	1.39
Standard deviation	1.3	0.05	0.02

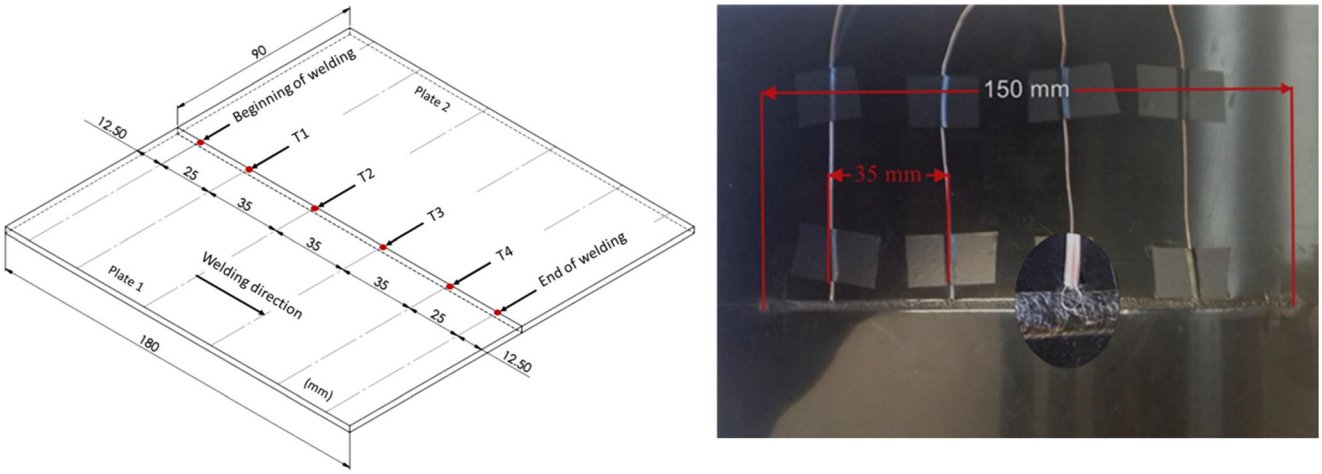

Fig. 3 Thermocouples position underneath the weld bead. **a** 3D drawing. **b** Welded plate

each in three levels using the Taguchi L9 orthogonal array, are presented in Table 2. In order to investigate the effect of the main process parameters on the weld strength, all experiments were repeated three times for averaging purposes according to the principles of Taguchi design. At the last repetition, the temperature beneath the weld nugget was measured and recorded. In this study, the ultimate tensile strength (UTS) of the joints was used to optimize the welding process according to the "the larger, the better" equation, which is the function proposed by Taguchi for signal-to-noise (S/N) ratio calculation:

$$S/N = -10\log\left(\frac{1}{n}\sum_{i=1}^{n}\frac{1}{y_i^2}\right) \quad (1)$$

Before the welding process, the abutting edges of plates were machined and straightened using a milling machine to guarantee a perfect surface contact between the two plates. After the welding process, three specimens were extracted by machining the welded plates perpendicular to the welding direction. Tensile tests were performed according to the ASTM Standard D638-2a [17]. The same standard was used to characterize the parent material in order to compare to the welds' ultimate tensile strength. Tensile tests were carried out with a speed of 5 mm/min in a MTS® 810 tensile testing machine [16]. Regarding data acquisition, a piezoelectric load cell with a maximum capacity of 10 kN and an MTS® clip gage extensometer were employed to measure strain. The mechanical properties of the parent material were obtained by testing five specimens following the ASTM standard, as presented in Table 3.

Due to the parent materials' low thermal conductivity, temperature sensors had to be located as near as possible to the weld bead. Thermocouples were calibrated before the welding process and were located beneath the weld nugget surface in four equally located positions as illustrated in Fig. 3, to investigate the generated heat at the bottom of the weld nugget. For this purpose, AD 595's ICs from Analog Devices® were employed as complete instrumentation amplifiers for K-type thermocouples with cold junction compensation and a gain of 247.3 (10 mV/°C divided by 40.44 μ V/°C) for amplifying and measuring the thermocouple electromotive force [18], as illustrated in Fig. 4a. The principal connections made for the AD 595s are shown in Fig. 4b. A dual power supply was provided with a symmetrical voltage of + 12/− 12 V, which supports temperature measurement for the entire range of the type-K thermocouples.

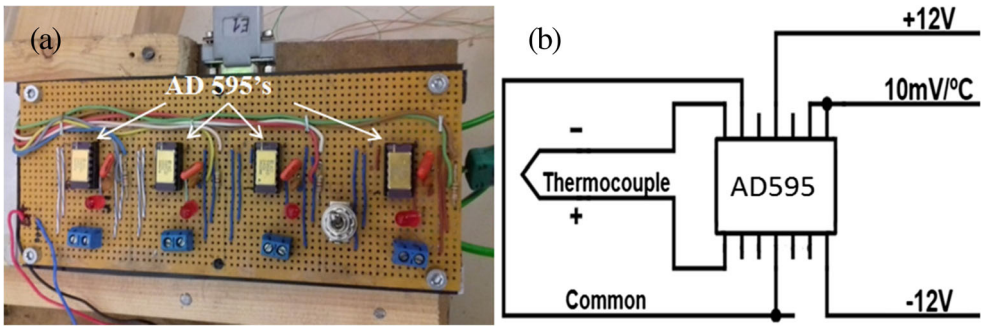

Fig. 4 **a** Conditioning circuit for thermocouples. **b** AD 595 main connections

Table 4 Joint efficiency obtained for each welding condition

Test number	Tool diameter (mm)	Rotational speed (rpm)	welding speed (mm/min)	Axial force (N)	Mean of the joint efficiency (%)		
					Trial 1	Trial 2	Trial 3
S1	3	1500	30	800	56.1	31.7	30.3
S2	3	2000	50	950	61.5	94.4	88.6
S3	3	2500	70	1100	90.8	94.8	96.9
S4	4	1500	50	1100	60.3	53.5	25.5
S5	4	2000	70	800	95.7	93.6	93.0
S6	4	2500	30	950	90.5	86.7	88.6
S7	5	1500	70	950	94.7	94.2	93.3
S8	5	2000	30	1100	76.9	85.0	86.1
S9	5	2500	50	800	96.7	97.3	90.4

3 Results and discussion

3.1 Joint efficiency

For comparing purposes, joint efficiency was introduced for each welded plate to classify the weld quality, which is a dimensionless numerical quantity. The results of the experimental tests are presented in Table 4. The base material's tensile strength was used as a reference to compare with the welded specimens for each set of welding parameters. Joint efficiency of each weld is achieved by dividing the tensile strength of each weld, S (x), by the parent material's tensile strength (S (0) = 921.7 N), as shown in Eq. 2. Three specimens were cut from each welded plate and tested, and the joint efficiency was calculated using the mean value of those three tests.

$$\text{Joint efficiency } (\%) = \frac{S\,(\mathrm{x})}{S\,(0)} \times 100 \tag{2}$$

The analysis of variance (ANOVA) enabled the identification of the welding parameters with the most influence on the welds' tensile strength. The ANOVA was performed using a level of significance of 5%. The results indicate that all the selected welding parameters have a statistically significant effect on the weld quality with a p value below 0.05, as illustrated in Table 5. One of the most valuable information extracted from ANOVA is the relative contribution of each parameter on the output of the process, which is presented in Table 5.

The overall contribution of the residual error was 20.4%, which can be explained due to uncontrollable factors such as the fact that the welding method is position controlled rather than force controlled, the misalignments between the plates interface, trajectory of the tool, vibrations, and the effects of the thermocouples on the weld quality [16]. The analysis of the mean effect, which is presented in Fig. 5, shows that the strong welds are obtained using high rotational speed, high welding speed, and large tool dimensions.

Using this tool, most of the frictional heat is generated in the dwelling stage, while the probe rotates after plunging, without advancing. The most influential welding parameter was rotational speed, which is responsible for most of the frictional heat by rotating inside the copper sleeve, and temperature readings support this claim (Table 6). Larger probe diameter generated more frictional heat as the contact area between the rotating probe and the sleeve was higher. Regarding the traverse speed, the joint strength was improved by increasing the traveling speed. After the tool reaches the desired temperature while dwelling, a low welding speed will cause excessive amount of heat on the base materials, originating weak joints. One of the remarkable points of this tool design was the capability of welding with higher welding speed by just changing the sleeve design and size [2]. For the axial force, there is an inflection as presented in Fig. 5, which shows that the medium value creates welds with the optimal result. Using the low value of the axial force is not adequate to forge the soft materials into the weld nugget, and a high axial force pushes down the soft materials excessively, creating a weld nugget thinner than the base material's thickness, which affects the weld quality.

Table 5 Analysis of variance and % contribution

Source	Degrees of freedom	Sum of squares	Mean square	F value	p value	Contribution percentage
Tool diameter (mm)	2	147,051	73,525	8.52	0.002	11.9
Rotational speed (rpm)	2	455,033	227,516	26.37	0.000	40.1
Welding speed (mm/min)	2	250,571	125,286	14.52	0.000	21.4
Axial force (N)	2	84,593	42,296	4.90	0.020	6.2
Residual error	18	155,292	8627	–	–	20.4
Total	26	1,092,540	–	–	–	–
Model summary	R-sq	R-sq (adj)	R-sq (pred)			
	85.79%	79.47%	68.02%			

Fig. 5 Main effects plot for mean

3.2 Failure analysis

The visual inspection of the welds is divided in three main approaches: (1) the top surface quality of the weld, (2) deformation of the welded plates due to the bending distortion, and (3) the bottom surface quality of the weld. To produce sound weld with a good surface quality, the copper sleeve should generate adequate amount of heat to form a layer of soft material at the top surface, which is pushed down by the stationary shoulder under the axial force. In those cases, the base material and the weld bead are difficult to distinguish, as shown in Fig. 6a. It is even more challenging to obtain a decent surface quality at the bottom of weld, due to formation of a root defect, Fig. 6b. The root defect refers to the non-welded section at the bottom of the weld nugget, and it affects the weld quality directly. It is essential that the welding tool has the capacity to generate enough heat along with a good stirring of the soften material.

The tested specimens failed in different behaviors, which were categorized by their elongations after reaching the ultimate tensile strengths. The first type of failure occurred when specimens were subjected to a sudden break under the loading condition with a lower extension when compared with parent material, as shown in Fig. 7. For this type of failure, despite a nonlinear deformation before failure during a 10-mm extension, this type of specimens presented a brittle behavior, when compared with the parent materials, where a continuous ductile behavior was found. Different failure behaviors are associated with the amount of the heat generated and the welding speed. These two factors are responsible for the fact that the produced joints have different failure behaviors, mainly at the bottom of welds where temperature did not reach the desired temperature, precluding achievement of a homogenous weld bead. However, it is worthy to note that failing in this behavior does not mean the produced joint suffers from defect formations. As an example, an S(3) specimen with 96.9% joint

Table 6 The measured temperature during welding

Test number	Tool diameter (mm)	Rotational speed (rpm)	Welding speed (mm/min)	Axial force (N)	Measured temperature (°C)			
					T_1	T_2	T_3	T_4
S1	3	1500	30	800	90	90	–	140
S2	3	2000	50	950	140	–	160	160
S3	3	2500	70	1100	90	–	150	160
S4	4	1500	50	1100	–	110	115	115
S5	4	2000	70	800	–	105	120	120
S6	4	2500	30	950	170	250	> 250	> 250
S7	5	1500	70	950	155	185	185	190
S8	5	2000	30	1100	> 250	> 250	> 250	> 250
S9	5	2500	50	800	250	–	–	> 250

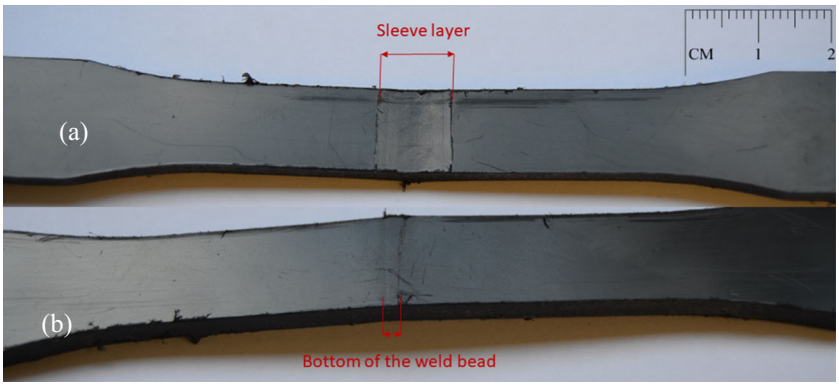

Fig. 6 Welded specimen with a good surface quality on top (**a**) and bottom (**b**) of the weld

efficiency revealed this behavior, as demonstrated in Fig. 7, where it is compared to the parent material's tensile strength.

The second failure type is referred to the welded specimens with the least elongation among other types, but with more ductility than the first type, as shown in Fig. 8. In this failure type, after a sudden break, the specimens continue to deform plastically. This behavior occurred as result of "sleeve layer" effect, which is corresponding to a thin layer of molten plastic due to passing of the hot sleeve on top of the weld nugget under the axial force. This layer showed a similar failure behavior to the parent material characteristics regarding the ability to deform plastically under tension. The thickness of the "sleeve layer" differs from weld to weld, depending on the generated heat and axial force. Two examples of this type of specimens after the tensile tests are presented in Fig. 8, where this type of failure is shown during the tensile tests, compared to the parent material.

The most ductile type of fracture corresponds to the welds with ability to deform plastically under tension, as demonstrated in Fig. 9. This deformation was not as much as the parent

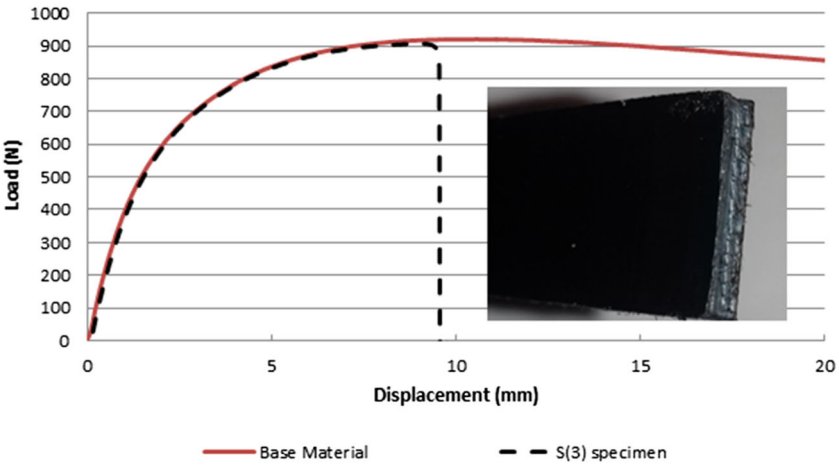

Fig. 7 Tensile strength result of S(3) welded specimen compared to the parent material

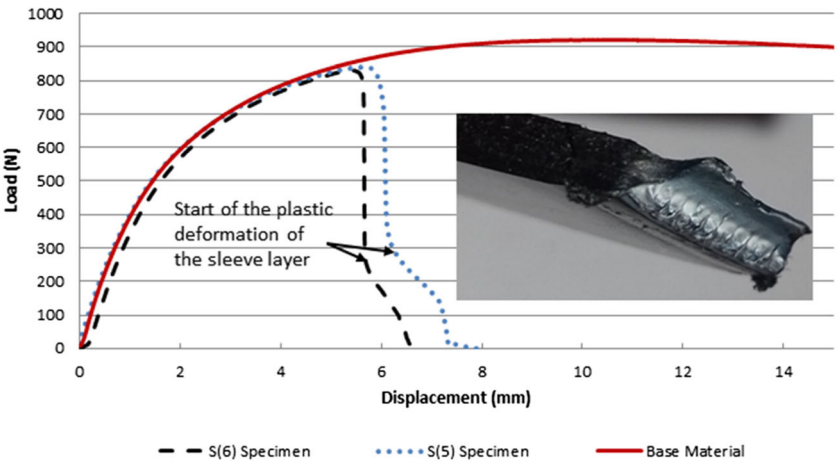

Fig. 8 Failure mode of the welded specimens with the least elongation, and the parent material

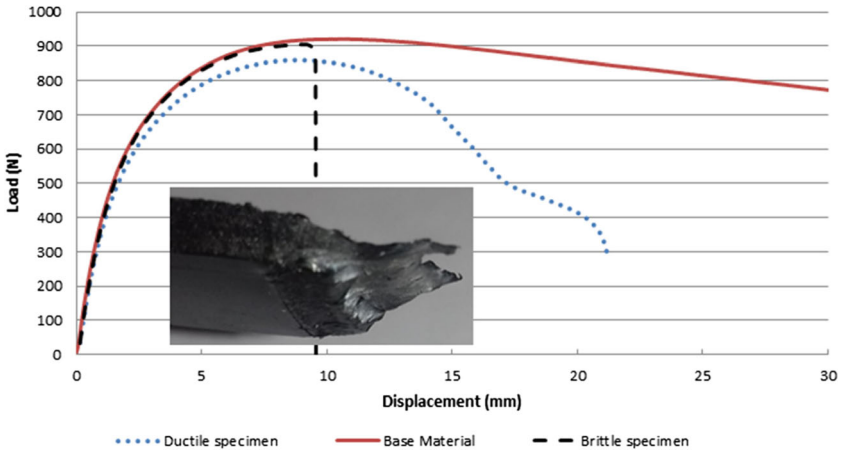

Fig. 9 Tensile test of specimen with ductile fracture, compared with base material and strongest specimen

material but nevertheless with more similarity than other types. This type of failure was the least common one and was found on the welds where the highest temperatures were applied beneath the weld nugget. The high welding temperature prevented formation of root defect, which might be the main reason for the sudden failure of the welded specimens. This type of failure occurred when the recorded temperature at the bottom of the weld exceeded 250 °C.

The rupture of the specimens occurred mainly in the retreating side of the weld, as presented in Fig. 10. This behavior is common for FSW of polymeric materials and can be explained by material flow and low thermal conductivity of polymers. As previous studies claimed, in the FSW process, the advancing sides are subjected to a higher temperature than the retreating sides of the welds, and low thermal conductivity of polymers magnifies this issue. This inadequate heat generation at the retreating side of the weld in comparison to the advancing side, caused the specimens to break from the retreating side [2]. However, using a stationary shoulder welding tool, it is very hard to prove the temperature differences on the different sides of the weld nugget.

3.3 Temperature measurement

Table 6 provides results for the temperature measurements, using four thermocouples (T1 to T4) for each welded plate. Some of the thermocouples were damaged when the tool was passing over them, introducing noise on the acquired measurements and made it difficult to analyze the data. The failed thermocouples are marked with "–" in Table 6. In some cases, it was possible to notice that the acquired temperature data recorded a temperature peek two or three times larger than average temperature being measured to that point. These abnormal measurements correspond to passing of the hot welding tool above the thermocouple under tool's high rotational speed and axial force. Predictably, the measured temperature of the welding tool is higher than the temperature beneath the weld bead, because of the frictional heat generated between the rotating probe and the copper sleeve. For some welding conditions, the recorded temperatures reached 250 °C, as shown in Table 6. In those cases, it was not possible to accurately differentiate whether the acquired temperature is corresponding to the temperature beneath the weld nugget or tip of the welding tool. For example, the S(8) set of parameters suffered the most from this unwanted behavior. The highest axial force and the lowest welding speed caused excessive amount of heat generation and forced the welding tool to pass very close to the thermocouple, which made it hard to separate temperature of the tool from the bottom of the welded plate.

Welding temperature measurement is a crucial factor to understand the welding process and the effect of the welding parameters on the heat generation. The majority of the acquired temperatures during this welding process were reliable and stable. As examples, the temperature readings of the thermocouple 4 of S(1) and thermocouple 2 of S(7) are presented in Figs. 11 and 12 respectively. The peak of the temperature indicates the moment, when the rotating probe was passing over the thermocouple located on the bottom of the welded plates. The comparison between the welding temperature and the parent material's melting temperature range (130–135 °C)

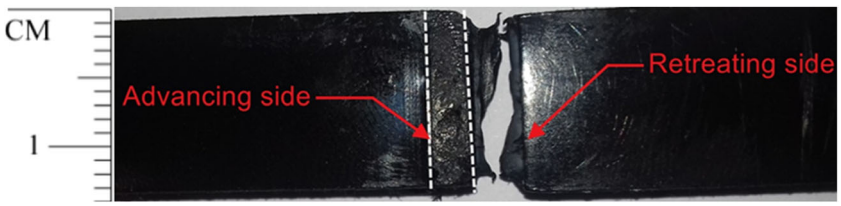

Fig. 10 Specimen fracture on the retreating side

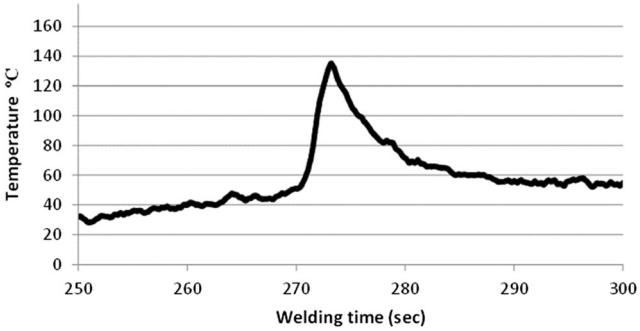

Fig. 11 Temperature readings test S(1), T4

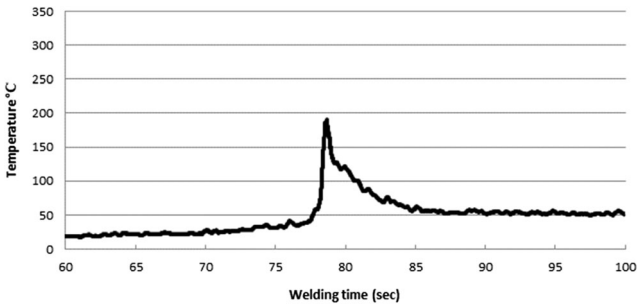

Fig. 12 Temperature readings test S(7), T2

confirms Strand's [19] claim that friction stir welding of polymers is not an absolute solid-state welding process, but a mixture of molten materials with a relatively small amount of solid materials.

For some welding conditions, it was possible to clearly differentiate between two different temperatures measured during welding. One of those values correlates to the measured temperature at the bottom of the weld bead, while the abnormal high temperature at the peak correlates to the welding tool when it is passing over the thermocouples. In order to clarify this abnormal temperature measurement at the bottom of the welded plates, a thermocouple was inserted into the copper sleeve to monitor the frictional heat generated inside the copper sleeve. This additional test was essential to clarify the peek temperature, which proves to be responsible for the recorded temperature of the welding tool.

The temperature of the tool was measured during an additional test, in order to confirm the magnitude difference between the temperatures on the weld bead and the tool during welding. This test was conducted with a 5-mm probe diameter, a rotational speed of 2500 rpm, a welding speed of 70 mm/min, and an axial force of 950 N. This parameter combination, especially tool diameter and tool rotational speed, is responsible for most of the heat generation on the copper sleeve. The temperature rises significantly during the dwell time, and the heat is transferred from the copper sleeve to the base material when advancing along the weld bead. The dwell time was enough for the tool to reach the desired temperature, which led to better weld quality using high welding speed. Using this tool and parameters, the low welding speed generated an excessive amount of heat, which affects the weld quality. Generally, using the proper sleeve size and welding parameters, it is possible to weld with much higher speed, even without a need of an external heat source. The temperature of the welding tool was measured by inserting a thermocouple inside the copper sleeve. High thermal conductivity of copper and the thermal isolation of the Teflon insured that this method was reliable to measure the temperature due to the generated frictional heat inside the welding tool.

Sleeve temperature reading shows that temperature increases rapidly during dwell time. The 10-s dwelling before traveling generates enough frictional heat for the sleeve to reach the desired temperature by rotating the probe inside the copper sleeve. Using the mentioned welding parameters, the temperature ranged between 350 and 400 °C, as shown in Fig. 13. The amount of heat generated between the rotating tool and the copper sleeve enables the base materials to preheat by the copper sleeve before passing of the rotating probe, which leads to strong welds without the need of an external heat source.

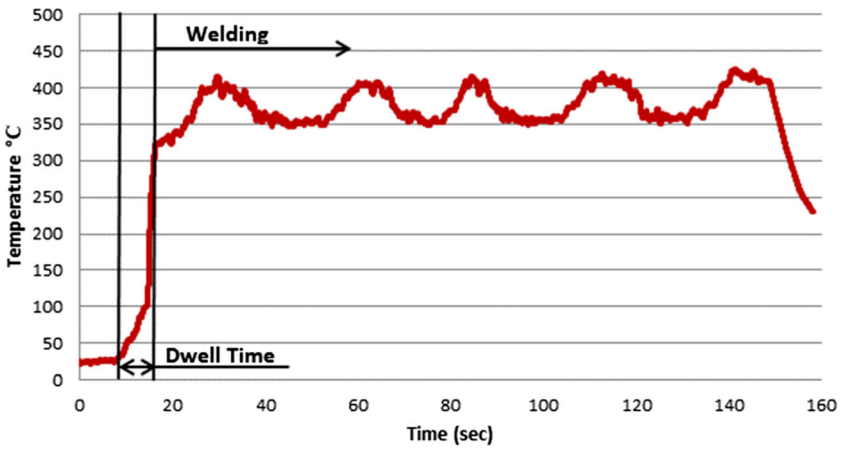

Fig. 13 Sleeve temperature readings with parameters selected for heat generation

4 Conclusions

In this study, the effect of FSW parameters on the weld quality was analyzed with the support of a Taguchi design of experiments and ANOVA methods. Also, the welding temperature was measured for each tested welding condition, in order to study the effect of the welding parameters and amount of the frictional heat generated by the developed welding tool. The welding temperature was measured by four thermocouples located beneath the weld nugget, and the sleeve temperature was monitored during the welding process by use of a thermocouple through the stationary shoulder inside the sleeve wall. Using this tool design concept, the frictional heat was generated by surface contact between the rotating probe and the copper sleeve under an axial force. As with all the friction stir welding processes, the optimal welding parameters are directly related to the welding tool design and its variables. It was concluded, with an appropriate tool design, sleeve size, and geometry, this tool is capable of producing strong welds with a good surface quality without the necessity of an external heat source. The maximum joint efficiency of 97% was obtained compared to the parent material's UTS.

The statistical analyses showed that all the input parameters had a statistically significant effect on the weld quality. Tool's rotational speed had the highest contribution (40%) followed by the welding speed (21%), tool diameter (12%), and axial force (6%). Strongest welds were obtained using high rotational speed and high welding speed, and an intermediate value for the axial force (950 N). Basically, measuring the sleeve temperature showed that during the dwell time, the rotational movements of the tool inside the copper sleeve generate most of the frictional heat, which made it possible to use a high welding speed to avoid excessive heat generation and material degradation. Three types of fractures occurred for different specimens, depending on the heat generation and welding parameters, which were categorized by the welded specimen's ductility and elongation after reaching their UTS.

Funding information Dr. Moreira acknowledges POPH – QREN-Tipologia 4.2 – Promotion of scientific employment funded by the ESF and MCTES. Authors gratefully acknowledge the funding of Project NORTE-01-0145-FEDER-000022 - SciTech - Science and Technology for Competitive and Sustainable Industries, cofinanced by Programa Operacional Regional do Norte (NORTE2020), through Fundo Europeu de Desenvolvimento Regional (FEDER). The funding provided by project Sold&Maq - Equipamento integrado de soldadura em estado sólido multimateriais e maquinagem NORTE-01-0247-FEDER-023694 is acknowledged.

References

1. Colligan KJ (2010) 2 - The friction stir welding process: an overview. Friction Stir Welding:15–41. https://doi.org/10.1533/9781845697716.1.15
2. Eslami S et al (2015) Effect of friction stir welding parameters with newly developed tool for lap joint of dissimilar polymers. Procedia Eng 114:199–207. https://doi.org/10.1016/j.proeng.2015.08.059
3. Eslami S, Tavares PJ, Moreira PMGP (2016) Friction stir welding tooling for polymers: review and prospects. Int J Adv Manuf Technol:1–14. https://doi.org/10.1007/s00170-016-9205-0
4. Eslami S et al (2018) Multi-axis force measurements of polymer friction stir welding. J Mater Process Technol 256:51–56. https://doi.org/10.1016/j.jmatprotec.2018.01.044
5. Mishra RS, Ma ZY (2005) Friction stir welding and processing. Mater Sci Eng R Rep 50:1–78. https://doi.org/10.1016/j.mser.2005.07.001
6. Eslami S et al (2015) Shoulder design developments for FSW lap joints of dissimilar polymers. J Manuf Process 20(Part 1):15–23. https://doi.org/10.1016/j.jmapro.2015.09.013
7. Besharati Givi MK, Asadi P (2014) 1 - General introduction. Adv Friction-Stir Weld Process:1–19. https://doi.org/10.1533/9780857094551.1
8. Thomas WM, Nicholas ED (1997) Friction stir welding for the transportation industries. Mater Des 18:269–273. https://doi.org/10.1016/S0261-3069(97)00062-9
9. Defalco J (2009) Friction stir process now welds steel pipe. Weld J 88:44–48
10. Nunes A (1998) Heat input and temperature distribution in friction stir welding. Month:163–172
11. Chao YJ, Qi X, Tang W (2003) Heat transfer in friction stir welding-experimental and numerical studies. J Manuf Sci Eng 125:138–145. https://doi.org/10.1115/1.1537741
12. Magalhães A (2016) Thermo-electric temperature measurements in friction stir welding: towards feedback control of temperature. University West
13. Golezani AS et al (2015) Elucidating of tool rotational speed in friction stir welding of 7020-T6 aluminum alloy. Int J Adv Manuf Technol 81:1155–1164. https://doi.org/10.1007/s00170-015-7252-6
14. Bozkurt Y (2012) The optimization of friction stir welding process parameters to achieve maximum tensile strength in polyethylene sheets. Mater Des 35:440–445. https://doi.org/10.1016/j.matdes.2011.09.008
15. Eslami S et al (2017) Parameter optimisation of friction stir welded dissimilar polymers joints. Int J Adv Manuf Technol:1–12. https://doi.org/10.1007/s00170-017-0043-5
16. Miranda JFC (2017) Nova ligação por FSW de materiais poliméricos
17. D638, A.S (2010) Standard test method for tensile properties of plastics. ASTM International. https://doi.org/10.1520/d0638-14
18. Gao J et al (2015) Improvements of mechanical properties in dissimilar joints of HDPE and ABS via carbon nanotubes during friction stir welding process. Mater Des 86:289–296. https://doi.org/10.1016/j.matdes.2015.07.095
19. Strand S (2003) Joining plastics-can friction stir welding compete? Electrical Insulation Conference and Electrical Manufacturing & Coil Winding Technology Conference, 2003. Proceedings. 321–326